Oxidized implants and their influence on the bone response

Y. T. SUL[1,2]* C. B. JOHANSSON[1], Y. JEONG[3], K. RÖSER[4], A. WENNERBERG[1] T. ALBREKTSSON[1].
[1]*Department of Biomaterials/Handicap Research, Institute for Surgical Science, University of Göteborg, Sweden*
[2]*Osseointegration Research Institute, Seoul, Korea*
[3]*Surface Engineering Department, Korea Institute of Machinery and Materials, 66 Sangnam-dong, Change 641-010, Korea*
[4]*Department of Oral Pathology, University of Hamburg, Martinistrase 52, D 20246 Hamburg, Germany*
E-mail: young-taeg.sul@hkf.gu.se

Surface oxide properties are regarded to be of great importance in establishing successful osseointegration of titanium implants. Despite a large number of theoretical questions on the precise role of oxide properties of titanium implants, current knowledge obtained from *in vivo* studies is lacking. The present study is designed to address two aspects. The first is to verify whether oxide properties of titanium implants indeed influence the *in vivo* bone tissue responses. The second, is to investigate what oxide properties underline such bone tissue responses. For these purposes, screw-shaped/turned implants have been prepared by electrochemical oxidation methods, resulting in a wide range of oxide properties in terms of: (i) oxide thickness ranging from 200 to 1000 nm, (ii) the surface morphology of barrier and porous oxide film structures, (iii) micro pore configuration – pore sizes $< 8\,\mu m$ by length, about $1.27\,\mu m^2$ to $2.1\,\mu m^2$ by area and porosity of about 12.7–24.4%, (iv) the crystal structures of amorphous, anatase and mixtures of anatase and rutile type, (v) the chemical compositions of TiO_2 and finally, (vi) surface roughness of 0.96–1.03 μm (Sa). These implant oxide properties were divided into test implant samples of Group II, III, IV and V. Control samples (Group I) were turned commercially pure titanium implants. Quantitative bone tissue responses were evaluated biomechanically by resonance frequency analysis (RFA) and removal torque (RT) test. Quantitative histomorphometric analyses and qualitative enzyme histochemical detection of alkaline (ALP) and acidic phosphatase (ACP) activities were investigated on cut and ground sections after six weeks of implant insertion in rabbit tibia. In essence, from the biomechanical and quantitative histomorphometric measurements we concluded that oxide properties of titanium implants, i.e. the oxide thickness, the microporous structure, and the crystallinity significantly influence the bone tissue response. At this stage, however, it is not clear whether oxide properties influence the bone tissue response separately or synergistically.

1. Introduction

Despite theoretical emphasis on the importance of surface oxide properties of the titanium implants for a successful osseointegration [1, 2], there is still a lack of knowledge of their role for the *in vivo* outcome. In fact, very few *in vivo* studies have been performed investigating the bone tissue responses to surface oxide properties of c.p. titanium implants [3–9]. Hazan *et al.* [3, 4] reported an increased shear strength by using heat-treated titanium implants in a rat model. Larsson *et al.* [5–7] found no major differences of the histomorphometric measurements between machined/anodized implants with an oxide thickness of 180–200 nm to machined implants with an oxide thickness of 3–5 nm in rabbit bone. Hanawa *et al.* [8] and Nishiguchi *et al.* [9], also reported an improved bone tissue response to the modified surface oxide by the ion implantation and the socking/heat treatment respectively.

Do the oxide properties of implant surfaces have an effect on osseointegration? If any, what oxide properties

* Author to whom correspondence should be addressed.

of the implant surface will play an important role during the dynamic osseointegration process?

Our earlier methodological studies for surface oxide preparation have indicated that the electrochemical growth behavior of the oxide film on c.p. titanium metal was strongly dependent on the anodic parameters such as the concentration of the electrolyte, the applied current density, the anodic forming voltage, the given temperature, the agitation speed, and the surface area ratios of cathode to anode [10]. By controlling such electrochemical parameters in a standardized manner, this study is designed to prepare a variety of surface oxide properties in terms of oxide thickness, surface topography, especially pore configurations (pore size, porosity, pore size distribution), crystal structure, chemical composition, and the surface roughness. The detailed characteristics of the surface oxide property employed in the present study will be published elsewhere [11] (the current paper is focusing on *in vivo* investigations).

2. Materials and methods

2.1. Implant preparation

Screw-shaped implants with pitch-height of 0.5 mm, an outer diameter of 3 mm, a total length of 7.2 mm, with a 3.2 mm square head and an inner threaded hole of 2 mm, were manually machined/turned from 5 mm rods of commercially pure titanium (ASTM Grade 1). Fig. 1 illustrates the design of the implant. This design allows biomechanical tests. Implants for histomorphometric specimen were specially designed with two different surfaces. Half of the implant circumference had an anodized surface (test surface), the other half had a non-modified, i.e. a turned/machined surface (control surface). This design of the implant allowed a direct comparison between test and control group surfaces in similar biological sites. For a comprehensive description of the electrochemical oxidation method used in the present study, we refer to our previous study [10]. In brief, all surface oxides were prepared by using a dc power supply at galvanostatic mode in 0.1 M acetic acid. Currents and voltages were continuously recorded at intervals of 0.5 s by an IBM computer interfaced with the power supply. All details of the surface characterizations of titanium implants in the present study will be published separately [11].

2.1.1. Characteristics of the surface oxide of the titanium implant

For convenience, the implant samples were divided into five groups in accordance with the surface oxide properties, which are summarized in Table I. In brief, the oxide thickness was 17 nm ($\pm$ 6) on the ''native'' oxide film of control Group I implants. The anodic oxide thickness for Group II implants was 202 nm ($\pm$ 53), Group III 608 nm ($\pm$ 127), Group IV 805 nm ($\pm$ 12) and the Group V implants had an anodic oxide thickness of 998 nm ($\pm$ 199) (Fig. 2). Measurements of the oxide thickness were performed at four different locations on the screws; one thread-top, one thread-valley, one thread-flank and in the bottom. The surface morphology showed two different types of microstructures: a nonporous barrier structure in Group I and II and a porous structure in Groups III–V (Fig. 3). The pore size was $\leq 8\,\mu$m in diameter in Groups III–V. The pore size distribution (PSD) measured by opening area increased with the applied forming voltage to each Group: 1.27 μm^2 in Group III, 1.53 μm^2 in Group IV, and 2.10 μm^2 in Group V. The porosity corresponded to 12.7%, 24.2%, and 18.7% respectively. The crystallinity of the titanium oxide was assigned to amorphous phase for Group I–III, anatase phase for Group IV (a mixture of anatase and rutile phase as analyzed by Raman spectroscopy) and a mixture of anatase and rutile phase for Group V as analyzed by thin-film X-ray diffractometry (TF-XRD). The chemical composition in all the Groups was mainly TiO_2 with small variation in traces such as C, Ca, Na, Si. The surface roughness was in the range of 0.83 μm ($\pm$ 0.32) (Group I) to 1.03 μm ($\pm$ 0.27) (Group III).

2.2. Animals and surgical technique

The experiment was approved by the local animal ethic committee at the University of Göteborg and followed the routine guidelines at the laboratories of Biomaterials/Handicap Research regarding anaesthesia, implant

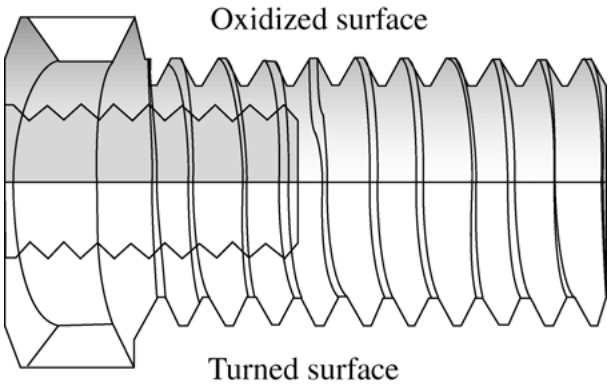

Figure 1 The implant was designed with a tetragonal head and an inner threaded part allowing biomechanical tests (RFA and RT). The samples used for histomorphometry, had two surfaces: one half (left side) is a turned native oxide surface and the other half (right side) is an electrochemically oxidized surface.

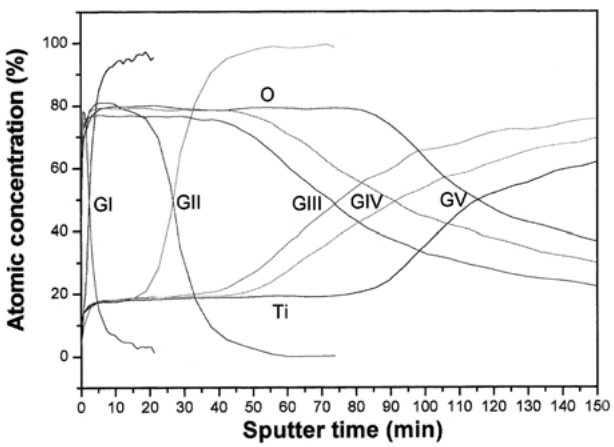

Figure 2 AES depth profiles shows the relative % distribution of titanium (Ti) and oxygen (O) (Gr I–V = Group I–V) ($E_p = 4.0\,\text{keV}, I_p = 300\,\text{nA}$).

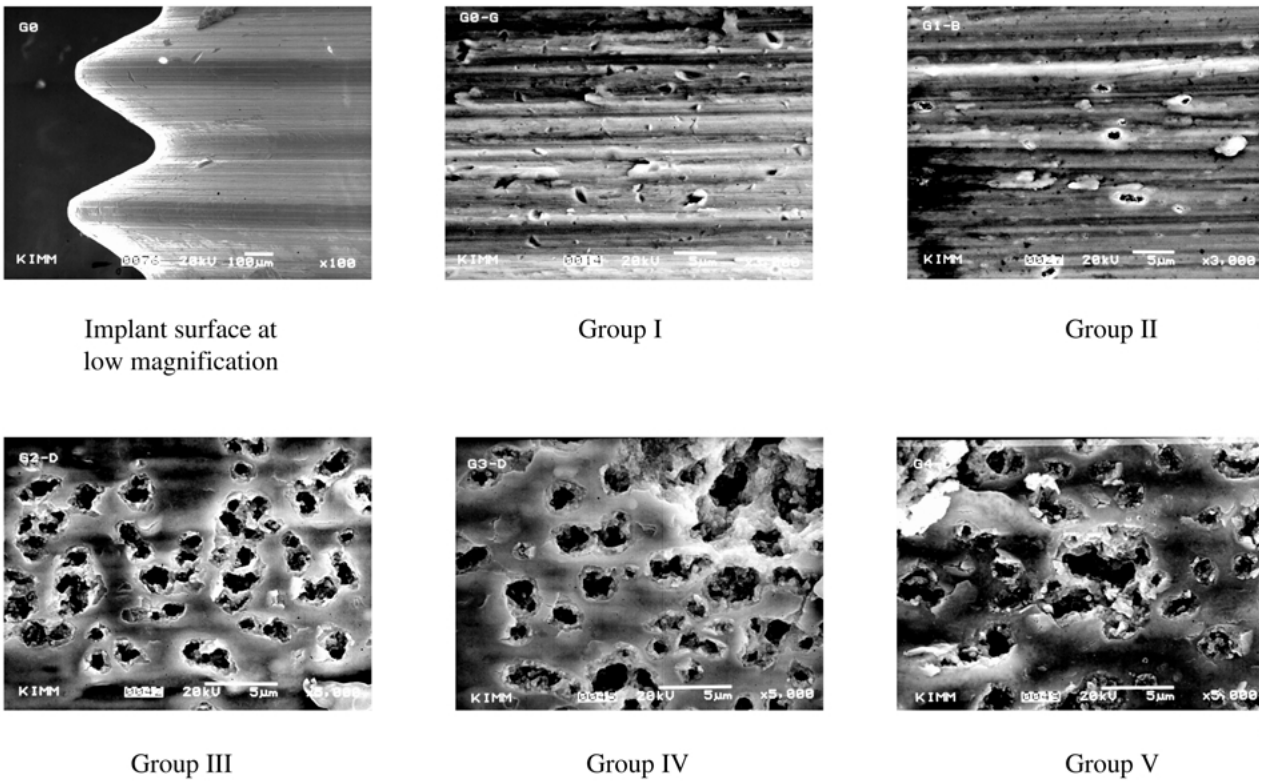

Figure 3 SEM pictures demonstrate two types of surface oxide structures: One structure is nonporous surface oxides in Groups I and II (× 3000). The other structure is porous surface oxides in Groups III–V (× 5000).

insertion and testing performed in the tibia of 12 rabbits. Four screw-shaped implants were randomly inserted in each tibia penetrating one cortical layer only. The two central implants were selected for biomechanical tests, whereas the most proximal and the most distal implant in each leg were processed for histomorphometrical tests. The implants were inserted in a pre-decided randomized design enabling multiple comparisons [12]. The follow-up time was six weeks. Eleven animals were sacrificed as pre-scheduled and one animal had to sacrificed earlier (two weeks) due to an unknown inflammation in the soft tissue around a control implant.

2.3. Specimen preparation and analysis

Resonance frequency analysis (RFA) and the peak removal torque (RT) measurements were performed on the two central implants. The remaining two implants were utilized for histomorphometrical and enzyme histochemical evaluations.

2.3.1. Resonance frequency analysis

This method is a non-destructive technique to demonstrate the implant stability and osseointegration in terms of interfacial stiffness (Hz) [13]. The resonance frequency was measured immediately after implant insertion and at sacrifice.

2.3.2. Removal torque test

The implant-to-bone integration, i.e. the stability of the bone bed, was evaluated with a destructive test, i.e. using an electrically controled RT unit, resulting in measurements of the peak RT (Nm) reflecting the interfacial shear strength at the time of sacrifice [14].

2.3.3. Histomorphometry and enzyme histochemistry

At sacrifice the non-RT tested implants were removed *en bloc* and immersed in fixative allowing later routine histological as well as enzyme histochemical investigation of alkaline (ALP) and acidic phosphatase (ACP) [15, 16].

Undecalcified cut and ground sections (10 µm thickness) were prepared in a standardized manner following the guidelines at the laboratories by using the Exakt® system [14, 17]. Computer-based histomorphometrical quantifications were performed in a light microscope. These measurements involved mean percentages of bone to metal contact (BMC) and the bone area in all threads as well as in the three best consecutive threads in the cortical region. Comparisons of the amount of bone inside the threads below the old cortex, i.e. endosteal bone tissue formation by osteoconduction, were also performed.

2.4. Statistics

The multiple comparison of statistical significance of RFA and RT test between all Groups was performed using two-way analysis of variance and the Tukey test. Statistical analyses of the histomorphometric data (paired control minus test) were performed using the Wilcoxon signed rank test. Differences were considered significant at $p < 0.05$.

TABLE I Summary of oxide growth parameters and surface characteristics of the five different types of c.p titanium implants

Oxide characteristics	Turned implants	Anodized implants			
	Group I	Group II	Group III	Group IV	Group V
Oxide growth constant		2.03 nm/V	3.04 nm/V	2.88 nm/V	2.63 nm/V
Oxide thickness[1]	17 ± 6 nm	202 ± 53 nm	608 ± 127 nm	805 ± 112 nm	998 ± 199 nm
Morphology[2]	Nonporous structure	Nonporous structure	Porous structure	Porous structure	Porous structure
Pore size distribution[3]		Negligable	1.27 ± 0.90 μm², ≤ 8 μm	1.53 ± 1.72 μm², ≤ 8 μm	2.10 ± 1.96 μm², ≤ 8 μm
Porosity[4]		Negligable	12.7 ± 3.6%	24.4 ± 3.7%	18.7 ± 5.2%
Crystallinity[5]	Amorphous	Amorphous	Amorphous	Anatase phase	Anatase and rutile phase
Chemical composition[6]	Primarily TiO_2 and traces; C, Ca, Na	Primarily TiO_2 and traces; C, Ca, Na, Si	Primarily TiO_2 and traces; C, Ca, Na, Si	Primarily TiO_2 and traces; C, Ca, Na, Si	Primarily TiO_2 and traces; C, Ca, Na, Si
Roughness (Sa)[7]	0.83 ± 0.32 μm	0.96 ± 0.34 μm	1.03 ± 0.33 μm	1.02 ± 0.27 μm	0.97 ± 0.30 μm

[1]Measured by continuous sputter etching with 4 keV Ar ion in Auger Electron Microscopy (AES) at four different locations of each implant; one thread-top, one thread-valley, one thread-flank and in the head of the screw implant.
[2]Characterized by scanning electron microscopy (SEM).
[3]Analyzed by image anlysis system-Bildanalyssystem AB® on negatives of the SEM pictures. PSD was presented by opening area and by diameter ($n = 3$, mean ± SD).
[4]Porosity presented a total area of the opening pores/a total of the scanned area-3 × 20 μm × 26 μm in% ($n = 3$, mean ± SD).
[5]Measured with TF-XRD and Raman spectroscopy complementarily.
[6]Performed with X-ray photoelectron spectroscopy (XPS) with both monochromatic and non-monochromatic X-ray sources.
[7]Measured with confocal laser scanning profilometer (TopScan3D®) with 245 μm × 245 μm of measuring area, on the three thread-tops, three thread-valleys, and three thread-flanks each, making 27 measurements for each group.

TABLE II Resonance frequency measurement (kHz) after six weeks of implant insertion

RFA (kHz)	Group I	Group II	Group III	Group IV	Group V
Implant #	9	9	8	9	9
Mean	6.99	6.999	7.092	7.055	7.236
SD	0.45	0.407	0.479	0.379	0.319

3. Results

3.1. Resonance frequency analysis

In general, the RFA showed an increasing trend with an increase of the oxide thickness (from Group I to Group V) after six weeks of implant insertion (Table II). However, there were no significant differences between the groups.

3.2. Removal torque test

In RT measurements (Fig. 4), the multiple comparison of the mean peak values of the RT using two-way analysis of variance and the Tukey test demonstrated that there were statistically significant differences between Group I compared to Group III–V implants; Group I revealed a mean of 0.075 Nm (± 0.29) compared to Group III with a mean of 0.113 Nm (± 0.042) $p = 0.023$. Group IV demonstrated a mean of 0.120 Nm (± 0.16) $p = 0.006$ and Group V demonstrated a mean of 0.129 Nm (± 0.022) $p = 0.001$ compared to Group I.

In addition, there were also statistically significant differences when comparing Group II to Groups III–V; Group II to Group III ($p = 0.044$), to Group IV ($p = 0.013$) and to Group V ($p = 0.002$). However, there were no statistically significant differences in RTs between Group I and II ($p = 0.999$), between Group III and IV, Group III and V, and Group IV and V ($p > 0.05$).

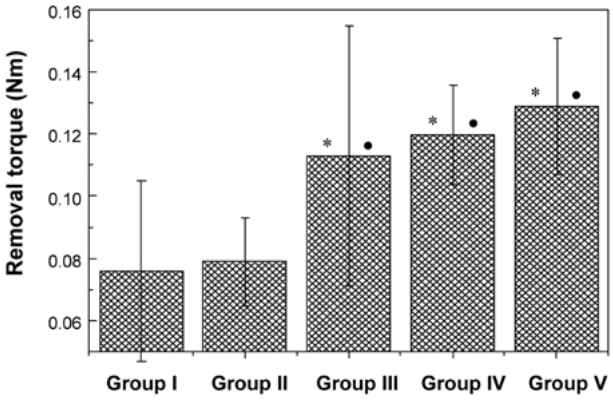

Figure 4 The peak RT measurements (Nm) after six weeks of healing time demonstrate statistically significant differences between Groups I and III, Groups I and IV, Groups I and V, Groups II and III, Groups II and IV, and Groups II and V. *$P < 0.05$ comparing Groups III–V to Group I. • $P < 0.05$ comparing Groups III–V to Group II.

3.3. Quantitative histomorphometrical evaluation on Toluidine blue stained cut and ground sections

3.3.1. Bone–metal contact

The BMC measurements in all implant threads of the test oxidized surface groups (Groups II–V) demonstrated greater mean values as compared to the paired control groups (Group I), but no significant differences ($p > 0.05$).

Comparisons of the bony contact in the three best consecutive threads in the cortical region between control and test groups, as shown in Fig. 5, revealed significant differences between Group I vs. Group IV ($p = 0.011$) and Group I vs. Group V ($p = 0.028$), but no significant differences between Group I vs. Group II ($p = 0.799$) or Group I vs. Group III ($p = 0.066$).

3.3.2. Bone area

There were no statistically significant differences when comparing the area measurements of control (Group I) to any of the test surfaces (Group II–V) ($p > 0.05$). The mean percentages of the bone area inside all implant threads were for all control turned surfaces 58% ($\pm$ 11, range 53–61). The four different test groups together revealed a mean of 60% ($\pm$ 10, range 59–64).

3.3.3. Newly formed bone

The amount of newly formed bone in all threads, revealed no statistically significant differences between control groups and the paired test Groups II–V ($p > 0.05$). However, as shown in Fig. 6, comparisons of the newly formed bone in the first endosteal thread below the old cortical bone (Fig. 7) demonstrated significant differences between Group I vs. Group III ($p = 0.017$) and Group I vs. Group IV ($p = 0.018$), but not significant between Group I vs. Group II ($p = 0.999$) and Group I vs. Group V ($p = 0.249$).

3.3.4. Qualitative enzyme histochemical detection of alkaline and acidic phosphatase activity

Irrespective of implant surface, the gross observations of the enzyme histochemical activity were similar based on the observation of a positivity for ALP (blue stained rims, indicative for bone formation) and ACP (red stained rims, indicative for bone resorption). However, the upper

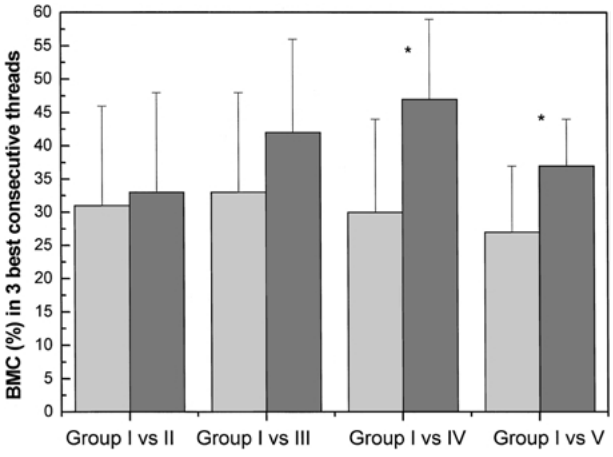

Figure 5 The comparisons of BMC in three best consective threads between test surfaces (Group II–V) and control surface (Group I) (*:$P < 0.05$).

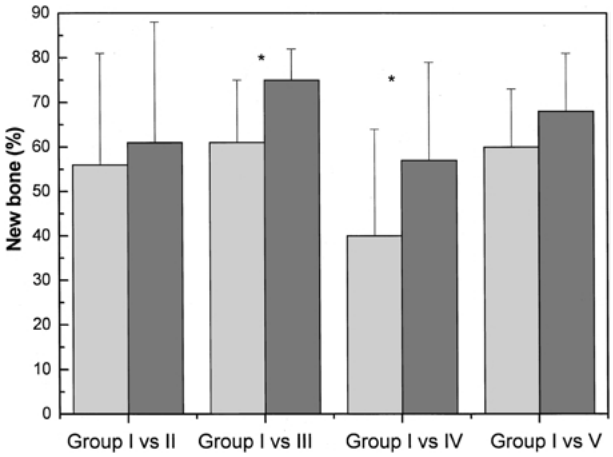

Figure 6 The comparisons of the newly formed bone in the first endosteal thread below the old cortex between test surfaces (Groups II–V) and control surface (Group I) (*$P < 0.05$).

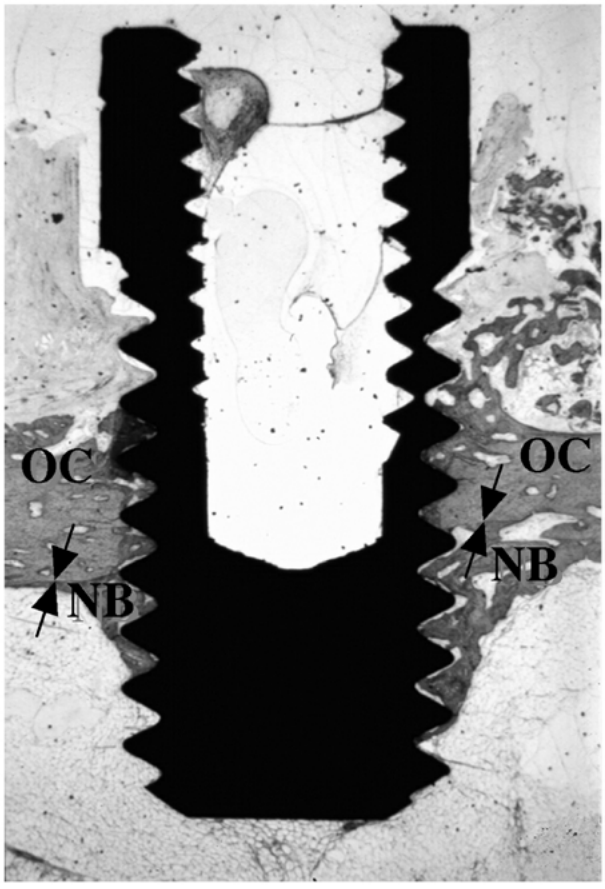

Figure 7 Cut and ground section of about 10 µm thickness stained with Toluidine-blue, after six weeks of implant insertion. Newly formed bone was distinguished by a demarcation line (arrows) between younger bone (dark staining) and older bone (pale staining). The original cortical bone (OC) is clearly visible as being paler stained compared to the new formed bone (NB)/younger bone which is darker stained. It is clearly visible that the amount of NB is greater on the test-oxidized-surface (right hand side). Magnification = there is a distance of 500 µm between the thread peaks.

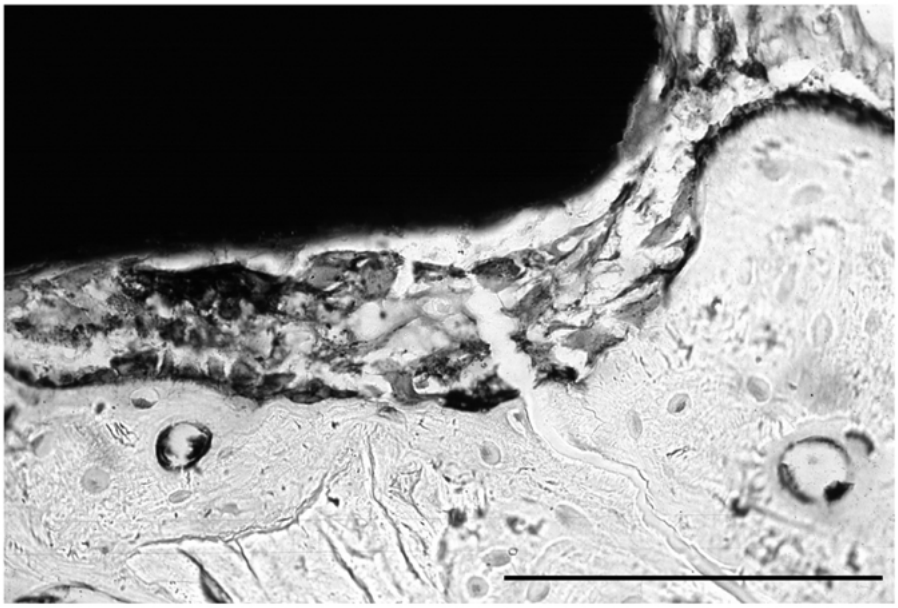

Figure 8 Bone remodeling cavity in close vicinity to the implant surface. One can observe coupling status of bone formation and bone resorption. Bar = 100 μm.

periosteal bone tissue formation revealed a greater activity for the ALP, i.e. a larger ongoing bone tissue formation was observed in this woven bone tissue region as compared to the endosteal part. Blue (ALP) and red (ACP) areas were observed seemingly overlapping – these areas indicated coupled bone formation (ALP positivity) and resorption (ACP positivity) (Fig. 8). The ALP activity was also well pronounced along the osteoblast layer immediately adjacent to the osteoide zone. In the marrow cavity, red stained multinucleated giant cells with green nuclei (counterstaining of methyl green) were often located in this area close to the implant surfaces.

4. Discussion

In essence, based on the RT and quantitative histomorphometric tests it seems evident that increasing the surface oxide thickness of titanium implants does result in simultaneous increase of the bone response. However, the explanation for this increased bone response may not be the increase of the oxide thickness *per se*, but rather changes in other surface parameters. We base this theory on the fact that increasing the surface oxide from about 3 to 200 nm thickness, when other surface parameters are unaltered, resulted in no measurable effects on the bone response in the studies by Larsson *et al*. [5–7] and in our investigation. However, it must be observed that there is another possible effect of increasing the oxide thickness, since Chen *et al*. [18] demonstrated that thermal oxidation of titanium increased its corrosion resistance. The change in surface roughness from the turned controls to the various oxidized test implants is only in the range of a tenth of a micrometer (Sa) and we find it unlikely that this small change in surface roughness alone can explain the outcome of our investigation. Chemical composition of the implants seemed to be quite similar in our different Groups I–V, and we find changes in chemical composition as an unlikely explanation for our findings. However, with surface oxides reinforced in the range of 600–1000 nm we see clear parallel changes in surface characteristics in form of altered microstructure (porosity) and the crystallinity of titanium oxide (anatase and rutile). Wong *et al*. [19] reported that bone matrix was deposited in pores of a size of 1–2 μm, resulting in higher push-out forces for such implants. The pore sizes in Groups III–V implants were in the same range as those in Wong's *et al*. [19] study. With respect to oxide crystallinity, McAlarney *et al*. [20] reported that *in vitro* C3 adsorption to anatase and rutile structures in thermally created oxides increased with increasing oxide thickness. However, Li [21] reported that bone showed a similar response to c.p. titanium and titania (rutile) in push out tests performed in a rabbit femoral model at one and three months after insertion. An ongoing separate study where we use a special technique to block the pores in Group III–V implants may, finally, help us to decide which one of the surface parameters that may explain our findings.

Our conclusion is that surface porosity and/or changed oxide crystallinity seem to be the most probable reasons for our findings of a greater bone response to implants with an oxide thickness of 600–1000 nm in comparison to those with only 3–200 nm thickness.

Acknowledgments

This study was supported by grants from the Hjalmar Svensson Research Foundation, the University of Göteborg, the Adlerbertska Research Foundation (Royal Society of Arts and Sciences in Göteborg), the Wilhelm and Martina Lundgren Foundation and the Swedish Medical Research Council.

References

1. B. KASEMO and J. LAUSMAA, in ''The Bone-Biomaterials Interface, Toronto'', edited by J. E. David (University of Toronto Press, 1991).
2. T. ALBREKTSSON, P. I. BRÅNEMARK, H. A. HANSSON, B. KASEMO, K. LARSSON, I. LUNDSTRÖM, D. MCQUEEN and R. SKALAK, *Ann. Biomed. Eng.* **11** (1983) 1.

3. R. HAZAN, R. BRENER and U. ORON, *Clin. Mater.* **7** (1991) 45.
4. R. HAZAN, R. BRENER and U. ORON, *Biomaterials* **14** (1993) 570.
5. C. LARSSON, P. THOMSEN, M. RODAHL, J. LAUSMAA, B. KASEMO and L. E. ERICSON, *Biomaterials* **15** (1994) 1062.
6. C. LARSSON, P. THOMSEN, B. O. ARONSSON, J. LAUSMAA, M. RODAHL and B. KASEMO, *ibid.* **15** (1996) 605.
7. C. LARSSON, L. EMANUELSSON, P. THOMSEN, L. E. ERICSON, B. O. ARONSSON, M. RODAHL, B. KASEMO and J. LAUSMAA, *J. Mater. Sci.: Mater. Med.* **8** (1997) 721.
8. T. HANAWA, Y. KAMIURA, S. YAMAMOTO, T. KOHGO, A. AMEMIYA, H. UKAI, K. MURAKAMI and K. ASAOKA, *J. Biomed. Mater. Res.* **36** (1997) 131.
9. S. NISHIGUCHI, T. NAKAMURA, M. KOBAYASHI, H.-Y. KIM, F. MIYAJI and T. KOKUBO, *Biomaterials* **20** (1999) 491.
10. Y.-T. SUL, C. B. JOHANSSON, Y. JEONG and T. ALBREKTSSON, *Med. Eng. Phys.* **23** (2001) 329.
11. Y.-T. SUL, C. B. JOHANSSON, S. PETRONIS, A. KROZER, Y. JEONG, A. WENNERBERG and T. ALBREKTSSON, *Biomaterials* (accepted) 2001.
12. H. Z. JERROLD, ''Biostatistical Analysis'', 2nd edition (Prentice-Hall International Inc., London, 1984).
13. N. MEREDITH (1997), Ph.D. thesis, Dept of Biomaterials/ Handicap Research, University of Göteborg, Sweden.
14. C. B. JOHANSSON (1991), Ph.D. thesis, Dept of Biomaterials/ Handicap Research, University of Göteborg, Sweden.
15. C.B. JOHANSSON, K. RÖSER, P. BOLIND, K. DONATH and T. ALBREKTSSON, *Clin. Impl. Dent. and Related Res.* **1** (2000) 33.
16. K. RÖSER, C. B. JOHANSSON, K. DONATH, T. ALBREKTSSON, *J. Biomed. Mater. Res.* **51** (2000) 280.
17. K. DONATH, *Der Präarator* **34**(1) (1988) 197.
18. G. F. CHEN, X. J. WEN, N. ZHANG, *Bio-Med. Mater. Eng.* **8** (1998) 61.
19. M. WONG, J. EULENBERGER, R. SCHENK and E. HUNZIKER, *J. Biomed. Mater. Res.* **29** (1995) 1567.
20. M. E. MCALARNEY, M. A. OSHIRO and C. V. MCALARNEY, *Int. J. Oral Maxillofac. Implants* **11** (1996) 73.
21. J. LI, *Biomaterials* **14** (1993) 229.

Received 14 May
and accepted 30 May 2001